Carbon-based perovskite solar cells by screen printing with preheating

Carbon-based perovskite solar cells by screen printing with preheating

V C Martinez[1], H Xie[2], A Mingorance[2], C Pereyra[2], A Narymany[2], and M M Gómez[1]*

[1]Faculty of Science, Universidad Nacional de Ingeniería, Av. Túpac Amaru 210, Lima 25, Peru

[2]Catalan Institute of Nanoscience and Nanotechnology, Bellaterra, Spain

*E-mail: mgomez@uni.edu.pe

Abstract. Carbon-based perovskite solar cells were manufactured by the screen-printing method using a triple mesoscopic layer of TiO_2, ZrO_2 and carbon. The perovskite solution was infiltrated at the TiO_2/ZrO_2 porous interface through the printed carbon layer on top of the ZrO_2. Using a simple preheating of the substrates and the perovskite solution, a film deposited in air can be obtained. Using this method, an air-processed CPSC made under a humid atmosphere with 55% RH achieved a PCE of 10.35%.

1. Introduction

Perovskite solar cells (PSCs) have attracted increasing research interest in the photovoltaics community since the first application of halide perovskite as a light-harvesting material in 2009 with a PCE of 3.8% [1]. Since then, PCE has increased dramatically, reaching the current record value of 23.7% [2]. This rapid evolution compared to all types of solar cells makes the PSCs a promising alternative for electricity production in the future. However, the use of expensive hole transport materials (usually spiro OMeTAD) and the contact of a thermally evaporated noble metal (such as Au or Ag) in conventional PSCs with the structure of FTO / compact-TiO_2 / m-TiO_2 / perovskite / HTM / Au [3] not only increases the cost of the devices but also affects their long-term stability [4]. Motivated by the need to solve these issues, after an intense experimental and research effort, carbon-based perovskite solar cells (CPSCs) without HTM were developed [5], and they have also shown the greatest stability among the PSCs [6]. Carbon materials, particularly graphite, carbon black and carbon nanotubes, have characteristics suitable for use as electrodes such as low cost, high electrical conductivity, availability, controllable porosity, chemical stability and being environmentally friendly. Due to these advantages, it is believed that carbon is the most promising material for use as an electrode.

The triple-layer mesoscopic structure can be manufactured using the screen-printing technique, which is a simple and economical technique that is promising for use in commercial production. A schematic cross section of a triple-layer, perovskite-based, fully printable mesoscopic solar cell (Fig. 1) shows that the mesoporous layers of TiO_2 and ZrO_2 were deposited on an F-doped SnO_2 (FTO)-covered glass sheet. The mesoporous layers were infiltrated with perovskite by drop-casting from solution through a carbon layer printed on top of the ZrO_2.

This work demonstrates a process to achieve the CPSCs in a triple-layer scaffold of TiO_2/ZrO_2/carbon to fabricate printable mesoscopic solar cells. The metal halide perovskite solution was infiltrated at the porous TiO_2/ZrO_2 interface through the printed carbon layer containing PbI_2 in Y-

butyrolactone together with methyl ammonium (MA) and cations of 5-aminovalent acid (5-AVA) as a solvent and using a preheating method for the perovskite's infiltration.

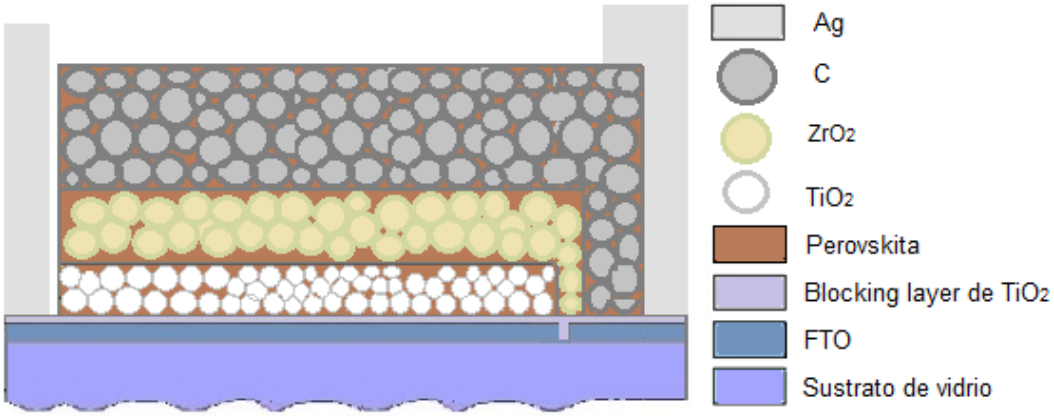

Figure 1. Schematic drawing showing the cross section of a triple-layer perovskite-based fully printable mesoscopic solar cell. The perovskite is infiltrated by the drop-casting method.

2. Experimental Section

In this section will be presented in detail how all the components of the mesoscopic solar cells were prepared.

2.1. Elaboration of layers

The etching process was carried out on a conductive substrate (SnO_2:F) with zinc powder and HCl. To clean the substrate, it was ultrasonically washed successively with detergent, distilled water, acetone, and ethanol. Further, the glasses were treated in an ultraviolet-ozone cleaning system for 10 min.
The compact TiO_2 layer (c-TiO_2) was deposited by a spray pyrolysis method at 300 °C with a solution of titanium diisopropoxide bis (acetylacetonate) (1.2 ml) dissolved in isopropanol (7.2 ml); it covered the whole surface, alternating between horizontal and vertical movements, and then, it naturally cooled to room temperature.

The mesoporous layers of titanium dioxide (TiO_2), zirconium oxide (ZrO_2) and carbon (C) were deposited by the screen-printing method. The TiO_2 paste was dissolved in anhydrous terpineol in a ratio of 2:3. Then, this paste was deposited on top of the compact layer by screen printing and a thermal treatment until 550 °C was carried out. The ZrO_2 spacer layer was printed on the top of the TiO_2 layer successively, and then, a thermal treatment until 400 °C was carried out. Finally, a mesoporous coal paste was printed on top of the substrate and aligned with the TiO_2 layer, and then, the films were sintered at 400 ° C for 30 minutes. The complete printing process was carried out in air. Fig. 2 shows the printed mesoporous layers in the order in which they were printed.

2.2. Perovskite preparation and infiltration

The perovskite solution was prepared from lead iodide (0.922 g, PbI_2, TCI Europe), methyl ammonium iodide (MAI, Dyesol, 0.314 g), 5-ammonium valeric acid iodide (5-AVAI, Dyesol, 0.014 g) and of ϒ-butyrolactone (GBL, Aldrich, 2.1 ml). To dissolve, it was dissolved and heated at 60 °C for approximately 2 hours.

Prior to the infiltration, the perovskite solution and the substrates were heated at 60 °C for 15 minutes on a hot plate, and this process was called the preheating method. Then, the solution (4.5 µL) was infiltrated by drop casting from the top of the carbon layer; for perovskite crystallization, the devices were dried at 50 °C for 4 h.

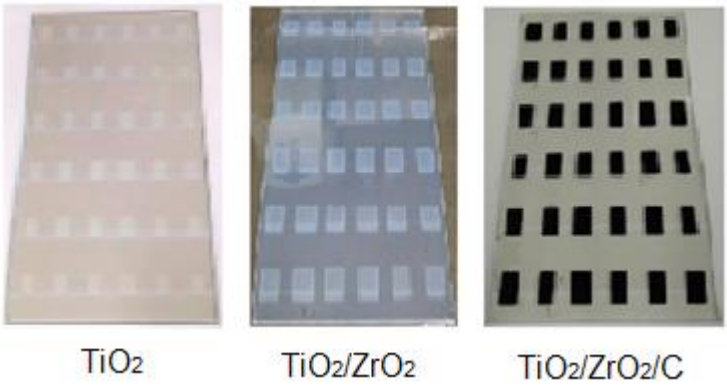

Figure 2. Mesoporous layers printed by the screen-printing method.

2.3. Contacts elaboration
Finally, the silver contacts are placed using a silver paste (Solaronix) that is spread with a baguette on the upper and lower edges of the cell, followed by a thermal treatment of 40 ºC for 1 h. All of the above procedures were completed in air atmosphere.

3. Results and discussion
In this section will be presented the optimization of the perovskite infiltration as well as the solar cell characterization using different techniques.

3.1. Optimization of the perovskite infiltration
To fabricate high-performance devices, a preheating of the perovskite solution and the substrates were carried out immediately prior to the infiltration at different temperatures varying from 30 °C (room temperature) to 90 °C. As presented in Fig. 3, the best results were obtained for the preheating at 50 and 60 °C, and to verify this outcome, we repeated the test using these two temperatures with 8 cells used for each temperature as shown in Fig. 4. It was found that higher PCE is obtained at 60 °C. Based on the results, we choose to heat the substrates and the solution to 60 °C for the perovskite solution infiltration.

The perovskite solution infiltration process is the most critical part of the work, and the infiltration of the perovskite solution with preheating reduces the ingress of oxygen and moisture during the perovskite deposition due to the increased vapor pressure of the solvent at higher temperatures [7], leading to good crystallization of the perovskite.

3.2. Device characterization
Mesoscopic solar cells were characterized by structural, morphological and electrical techniques as it is presented below.

3.2.1. X-ray diffraction
X-ray diffraction (XRD) measurements were performed for the devices to characterize perovskite growth when infiltration was realized at 30 °C and 60 °C, with the obtained results presented in Fig. 5. The (110), (220) and (310) peaks are attributed to the $CH_3NH_3PbI_3$ perovskite structure [8], and using Scherrer equation, the crystal size is obtained as approximately 60 nm. * represents the peak of the carbon and # represents the (001) peak due to PbI_2 [8]. The XRD measurements were performed using a Malvern PANalytical instrument using Cu K_α ($\lambda = 0.154$ nm) radiation.

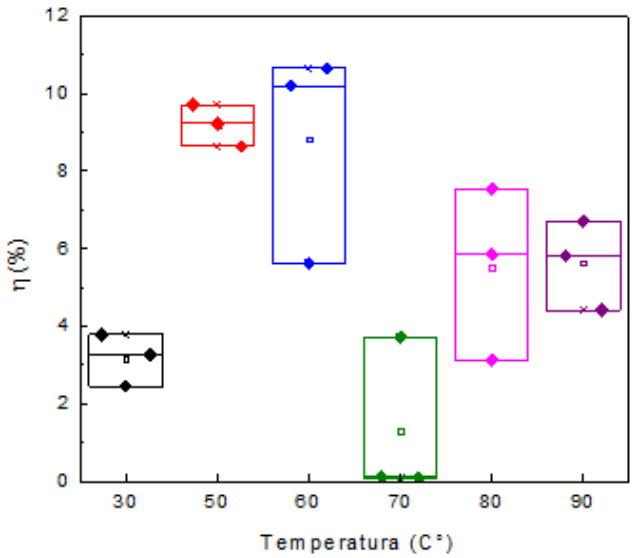

Figure 3. Efficiencies of the preheating to different temperatures for perovskite infiltration

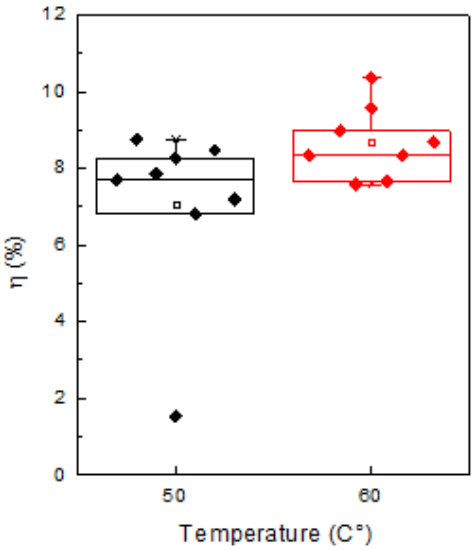

Figure 4. Efficiencies with preheating at 50 °C and 60 °C.

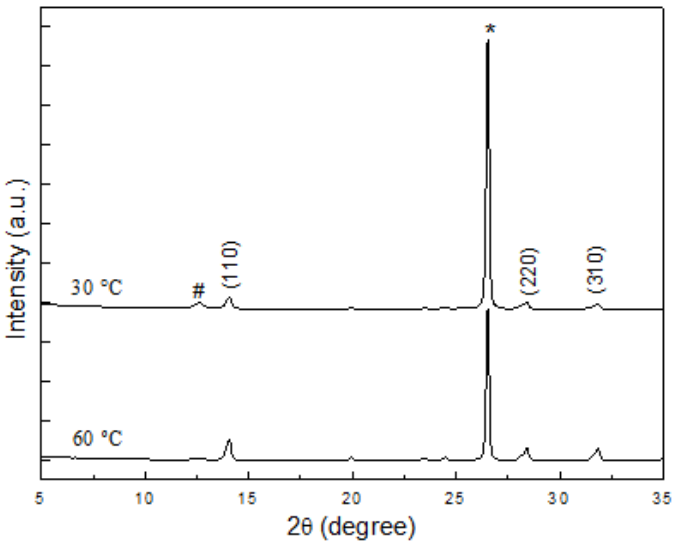

Figure 5. X-ray diffraction patterns of the devices with perovskite infiltration at 30 °C and 60 °C, where the (110), (220) and (310) peaks belong to the perovskite $CH_3NH_3PbI_3$, * represents the peak of the carbon and # represents the (001) peak of PbI_2.

3.2.2. Ultraviolet-visible and photoluminescence spectroscopy

For ultraviolet-visible (UV-vis) spectroscopy, to avoid the interference caused by the carbon layer, the precursor was infiltrated in the m-TiO_2/ZrO_2 scaffold. Due to the heating of the device to 60 °C, the absorption of the perovskite was considerably enhanced (Fig. 6). Considering the two samples, an onset of absorption is observed at 750 nm, matching the result for the typical tetragonal perovskite phase of $CH_3NH_3PbI_3$ [9], and the obtained bandgap is 1.65 eV. The UV-vis analyses of films were carried out using a Varian Cary 4000 spectrophotometer.

Photoluminescence (PL) spectra of TiO_2/ZrO_2/intermediate were measured to correlate the quality of the perovskite absorber in the scaffold with the heating of the substrates. Upon heating, the peak intensity at 783 nm increased significantly, but no distinguishable peak shift was observed in the steady-state PL spectra (Fig. 7). These spectra were obtained using an Andor spectrometer.

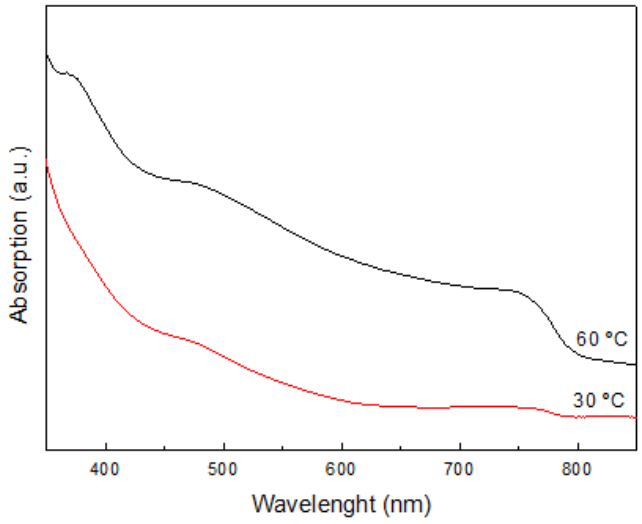

Figure 6. UV-vis spectra of the infiltrated perovskite solution in the m-TiO_2 / m-ZrO_2 layer at 30 °C and 60 °C.

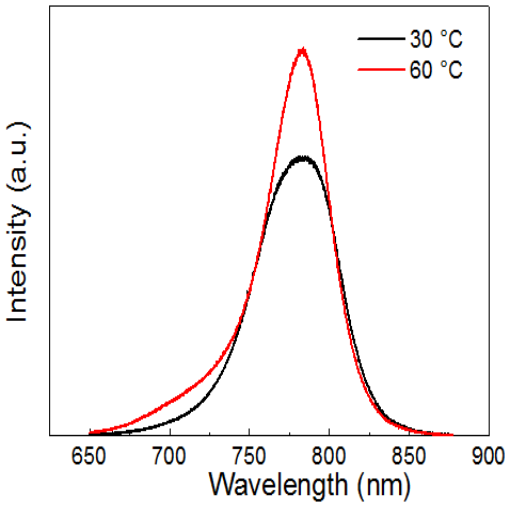

Figure 7. Steady-state PL spectra of the infiltrated perovskite solution in the m-TiO_2 / m-ZrO_2 layer at 30 °C and 60 °C.

3.2.3. Scanning electron microscopy

A scanning electron microscopy (SEM) image of the cross-section of the triple-layer, perovskite-based, printable mesoscopic solar cell (Fig. 8) shows that the mesoporous TiO_2 and ZrO_2 layers have thicknesses of ~150 and 400 nm, respectively, and were deposited on an F-doped SnO_2 (FTO) covered glass sheet. The mesoporous layers were infiltrated with perovskite by drop casting from solution through a 20 µm thick carbon layer printed on top of the ZrO_2 layer. The cross-section image of the cell was obtained using a Quanta FEI 650 FEG instrument.

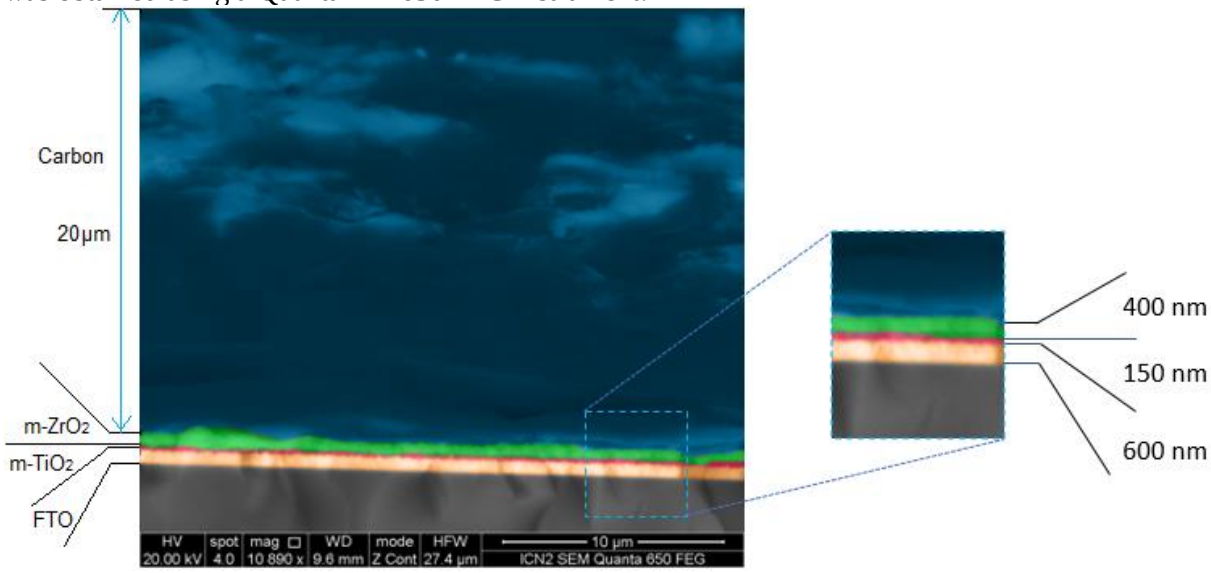

Figure 8. Cross-sectional SEM of the perovskite-infiltrated TiO_2/ZrO_2/carbon shelf.

3.3. Current density - voltage measurements:Characteristic curve current density - voltage (J-V)

Based on the above-described results, the next batch of devices were fabricated using the optimal perovskite infiltration method. The best obtained efficiency was 10.35%. The Steuernagel Solarkonstant

KHS1200 instrument equipped with an AM1.5 filter and calibrated with a Zipp & Konen CM-4 bolometric pyranometer was used. The J-V curves were measured using a Keithley 2601 multimeter.

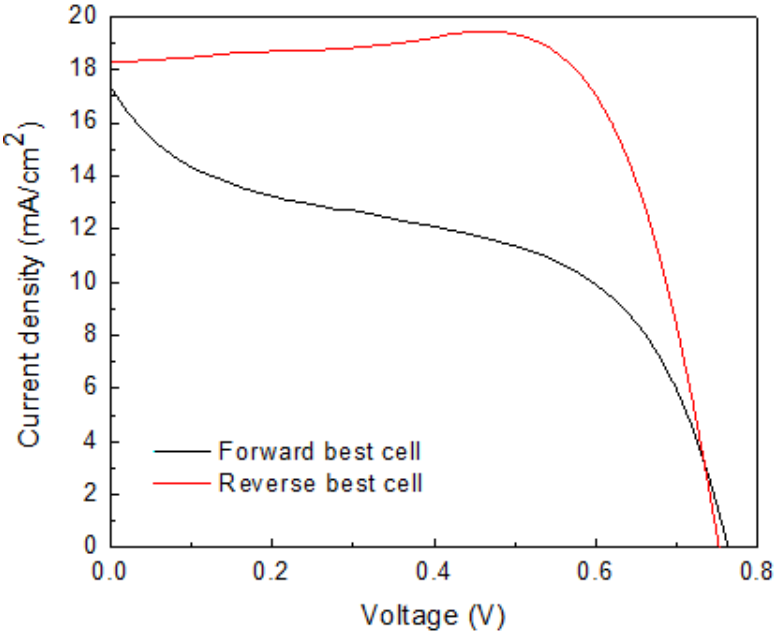

Figure 9. Characteristic curve *J-V* of the average of cells and the forward and reverse biases of the best cell.

Table 1 presents the values obtained from the prepared cells.

Table 1. Characteristic values of the cells obtained with preheating at 60 °C.

	Ƞ (%)	*Voc* (V)	*Jsc* (mA/cm^2)	*FF* (%)
1	7.65	0.66	17.75	65.12
2	7.58	0.69	19.13	56.99
3	9.57	0.71	19.26	69.50
4	8.97	0.69	19.32	67.46
5	8.34	0.72	18.21	63.75
6	10.35	0.75	18.29	75.33
7	8.34	0.71	15.20	77.68
8	8.69	0.76	16.80	67.78

4. Conclusions

A simple preheating method is employed to fabricate high-efficiency CPSC in ambient air with RH of 55%. This preheating method evaporates the absorbed moisture and oxygen from the substrate and the GBL solvent, thus forming an environment to screen the ingress of water and oxygen molecules from the ambient air onto the perovskite area.

Using perovskite films made with preheating to 60 °C, we obtained high-efficiency PSCs with the highest efficiency of 10.35%.

Acknowledgments
One of the authors (V.M.) wish to acknowledge the scholarship by FONDECYT within the Doctoral Program in Sciences with mention in Energy from the National University of Engineering. The Peruvian National Council for Science and Technology (CONCYTEC) (Contract N° 024-2016-FONDECYT) is gratefully acknowledged for its financial support.

References
[1] A. Kojima, K. Teshima, Y. Shirai, T. Miyasaka, J. Am. Chem. Soc. 131 (2009) 6050.
[2] H.S. Kim, A. Hagfeldt, N.G. Park, Roy. Soc. of Chem. (2018).
[3] J. Burschka, N. Pellet, S.J. Moon, R. Humphry-Baker, P. Gao, M.K. Nazeeruddin, M. Gratzel, Nature 499 (2013) 316.
[4] H. Zhou, Q. Chen, G. Li, S. Luo, T.B. Song, H.S. Duan, Z. Hong, J. You, Y. Liu, Y. Yang, Science 345 (2014) 542.
[5] A. Mei, X. Li, Linfeng Liu, Z. Ku, T. Liu, Yaoguang Rong, M. Xu, M. Hu, J. Chen, Y. Yang, M. Grätzel, H. Han, Science 345 (2014) 295.
[6] G. Grancini, C. Roldan-Carmona, I. Zimmermann, E. Mosconi, X. Lee, D. Martineau, S. Narbey, F. Oswald, F. De Angelis, M. Graetzel, M.K. Nazeeruddin, Nature communications 8 (2017) 15684.
[7] Y. Cheng, X. Xu, Y. Xie, H.-W. Li, J. Qing, C. Ma, C.-S. Lee, F. So, S.-W. Tsang, Solar RRL 1 (2017) 1700097.
[8] Z. Song, S.C. Watthage, A.B. Phillips, B.L. Tompkins, R.J. Ellingson, M.J. Heben, Am. Chem. Soc. 27 (2015) 4612−19.
[9] T. Baikie, Y. Fang, J.M. Kadro, M. Schreyer, F. Wei, S.G. Mhaisalkar, M. Graetzel, T.J. White, J. Mat. Chem. A 1 (2013) 5628.